BELLE-CONF-0107

Observation of Color-Suppressed $\overline{B}^0 \to D^{(*)0}X^0$ Decays

The Belle Collaboration

Abstract

We report the first observation of color-suppressed $\overline{B}^0 \to D^0\pi^0$ and $D^{(*)0}\omega$ decays and evidence of $\overline{B}^0 \to D^{*0}\pi^0$ and $D^{(*)0}\eta$. The branching fractions are found to be $\mathcal{B}(\overline{B}^0 \to D^0\pi^0) = (2.9\ ^{+0.4}_{-0.3} \pm 0.6) \times 10^{-4}$, $\mathcal{B}(\overline{B}^0 \to D^0\omega) = (1.7\ ^{+0.5\ +0.3}_{-0.4\ -0.4}) \times 10^{-4}$, and $\mathcal{B}(\overline{B}^0 \to D^{*0}\omega) = (3.4\ ^{+1.3}_{-1.1} \pm 0.8) \times 10^{-4}$. The analysis is based on a data sample of 21.3 fb^{-1} collected at the $\Upsilon(4S)$ resonance by the Belle detector at the KEKB e^+e^- collider.

K. Abe[9], K. Abe[37], R. Abe[27], I. Adachi[9], Byoung Sup Ahn[15], H. Aihara[39], M. Akatsu[20], K. Asai[21], M. Asai[10], Y. Asano[44], T. Aso[43], V. Aulchenko[2], T. Aushev[13], A. M. Bakich[35], E. Banas[25], S. Behari[9], P. K. Behera[45], D. Beiline[2], A. Bondar[2], A. Bozek[25], T. E. Browder[8], B. C. K. Casey[8], P. Chang[24], Y. Chao[24], K.-F. Chen[24], B. G. Cheon[34], R. Chistov[13], S.-K. Choi[7], Y. Choi[34], L. Y. Dong[12], J. Dragic[18], A. Drutskoy[13], S. Eidelman[2], V. Eiges[13], Y. Enari[20], C. W. Everton[18], F. Fang[8], H. Fujii[9], C. Fukunaga[41], M. Fukushima[11], A. Garmash[2,9], A. Gordon[18], K. Gotow[46], H. Guler[8], R. Guo[22], J. Haba[9], H. Hamasaki[9], K. Hanagaki[31], F. Handa[38], K. Hara[29], T. Hara[29], N. C. Hastings[18], H. Hayashii[21], M. Hazumi[29], E. M. Heenan[18], Y. Higasino[20], I. Higuchi[38], T. Higuchi[39], T. Hirai[40], H. Hirano[42], T. Hojo[29], T. Hokuue[20], Y. Hoshi[37], K. Hoshina[42], S. R. Hou[24], W.-S. Hou[24], S.-C. Hsu[24], H.-C. Huang[24], Y. Igarashi[9], T. Iijima[9], H. Ikeda[9], K. Ikeda[21], K. Inami[20], A. Ishikawa[20], H. Ishino[40], R. Itoh[9], G. Iwai[27], H. Iwasaki[9], Y. Iwasaki[9], D. J. Jackson[29], P. Jalocha[25], H. K. Jang[33], M. Jones[8], R. Kagan[13], H. Kakuno[40], J. Kaneko[40], J. H. Kang[48], J. S. Kang[15], P. Kapusta[25], N. Katayama[9], H. Kawai[3], H. Kawai[39], Y. Kawakami[20], N. Kawamura[1], T. Kawasaki[27], H. Kichimi[9], D. W. Kim[34], Heejong Kim[48], H. J. Kim[48], Hyunwoo Kim[15], S. K. Kim[33], T. H. Kim[48], K. Kinoshita[5], S. Kobayashi[32], S. Koishi[40], H. Konishi[42], K. Korotushenko[31], P. Krokovny[2], R. Kulasiri[5], S. Kumar[30], T. Kuniya[32], E. Kurihara[3], A. Kuzmin[2], Y.-J. Kwon[48], J. S. Lange[6], S. H. Lee[33], C. Leonidopoulos[31], Y.-S. Lin[24], D. Liventsev[13], R.-S. Lu[24], D. Marlow[31], T. Matsubara[39], S. Matsui[20], S. Matsumoto[4], T. Matsumoto[20], Y. Mikami[38], K. Misono[20], K. Miyabayashi[21], H. Miyake[29], H. Miyata[27], L. C. Moffitt[18], G. R. Moloney[18], G. F. Moorhead[18], N. Morgan[46], S. Mori[44], T. Mori[4], A. Murakami[32], T. Nagamine[38], Y. Nagasaka[10], Y. Nagashima[29], T. Nakadaira[39], T. Nakamura[40], E. Nakano[28], M. Nakao[9], H. Nakazawa[4], J. W. Nam[34], Z. Natkaniec[25], K. Neichi[37], S. Nishida[16], O. Nitoh[42], S. Noguchi[21], T. Nozaki[9], S. Ogawa[36], T. Ohshima[20], Y. Ohshima[40], T. Okabe[20], T. Okazaki[21], S. Okuno[14], S. L. Olsen[8], H. Ozaki[9], P. Pakhlov[13], H. Palka[25], C. S. Park[33], C. W. Park[15], H. Park[17], L. S. Peak[35], M. Peters[8], L. E. Piilonen[46], E. Prebys[31], J. L. Rodriguez[8], N. Root[2], M. Rozanska[25], K. Rybicki[25], J. Ryuko[29], H. Sagawa[9], Y. Sakai[9], H. Sakamoto[16], M. Satapathy[45], A. Satpathy[9,5], S. Schrenk[5], S. Semenov[13], K. Senyo[20], Y. Settai[4], M. E. Sevior[18], H. Shibuya[36], B. Shwartz[2], A. Sidorov[2], S. Stanič[44], A. Sugi[20], A. Sugiyama[20], K. Sumisawa[9], T. Sumiyoshi[9], J.-I. Suzuki[9], K. Suzuki[3], S. Suzuki[47], S. Y. Suzuki[9], S. K. Swain[8], H. Tajima[39], T. Takahashi[28], F. Takasaki[9], M. Takita[29], K. Tamai[9], N. Tamura[27], J. Tanaka[39], M. Tanaka[9], Y. Tanaka[19], G. N. Taylor[18], Y. Teramoto[28], M. Tomoto[9], T. Tomura[39], S. N. Tovey[18], K. Trabelsi[8], T. Tsuboyama[9], T. Tsukamoto[9], S. Uehara[9], K. Ueno[24], Y. Unno[3], S. Uno[9], Y. Ushiroda[9], S. E. Vahsen[31], K. E. Varvell[35], C. C. Wang[24], C. H. Wang[23], J. G. Wang[46], M.-Z. Wang[24], Y. Watanabe[40], E. Won[33], B. D. Yabsley[9], Y. Yamada[9], M. Yamaga[38], A. Yamaguchi[38], H. Yamamoto[8], T. Yamanaka[29], Y. Yamashita[26], M. Yamauchi[9], S. Yanaka[40], M. Yokoyama[39], K. Yoshida[20], Y. Yusa[38], H. Yuta[1], C. C. Zhang[12], J. Zhang[44], H. W. Zhao[9], Y. Zheng[8], V. Zhilich[2], and D. Žontar[44]

[1]Aomori University, Aomori
[2]Budker Institute of Nuclear Physics, Novosibirsk
[3]Chiba University, Chiba
[4]Chuo University, Tokyo
[5]University of Cincinnati, Cincinnati OH

[6]University of Frankfurt, Frankfurt
[7]Gyeongsang National University, Chinju
[8]University of Hawaii, Honolulu HI
[9]High Energy Accelerator Research Organization (KEK), Tsukuba
[10]Hiroshima Institute of Technology, Hiroshima
[11]Institute for Cosmic Ray Research, University of Tokyo, Tokyo
[12]Institute of High Energy Physics, Chinese Academy of Sciences, Beijing
[13]Institute for Theoretical and Experimental Physics, Moscow
[14]Kanagawa University, Yokohama
[15]Korea University, Seoul
[16]Kyoto University, Kyoto
[17]Kyungpook National University, Taegu
[18]University of Melbourne, Victoria
[19]Nagasaki Institute of Applied Science, Nagasaki
[20]Nagoya University, Nagoya
[21]Nara Women's University, Nara
[22]National Kaohsiung Normal University, Kaohsiung
[23]National Lien-Ho Institute of Technology, Miao Li
[24]National Taiwan University, Taipei
[25]H. Niewodniczanski Institute of Nuclear Physics, Krakow
[26]Nihon Dental College, Niigata
[27]Niigata University, Niigata
[28]Osaka City University, Osaka
[29]Osaka University, Osaka
[30]Panjab University, Chandigarh
[31]Princeton University, Princeton NJ
[32]Saga University, Saga
[33]Seoul National University, Seoul
[34]Sungkyunkwan University, Suwon
[35]University of Sydney, Sydney NSW
[36]Toho University, Funabashi
[37]Tohoku Gakuin University, Tagajo
[38]Tohoku University, Sendai
[39]University of Tokyo, Tokyo
[40]Tokyo Institute of Technology, Tokyo
[41]Tokyo Metropolitan University, Tokyo
[42]Tokyo University of Agriculture and Technology, Tokyo
[43]Toyama National College of Maritime Technology, Toyama
[44]University of Tsukuba, Tsukuba
[45]Utkal University, Bhubaneswer
[46]Virginia Polytechnic Institute and State University, Blacksburg VA
[47]Yokkaichi University, Yokkaichi
[48]Yonsei University, Seoul

The decay modes $\overline{B}^0 \to D^{(*)0}X^0$, where X^0 is a light neutral meson, proceed via an internal spectator diagram and are expected to be suppressed relative to the external diagram, since the color of the $\overline{u}$ antiquark produced by the weak current must complement the color of the c quark as shown in Fig. 1. Studies of such color-suppressed decay modes can be used to test models of hadronic B meson decays and provide information on final-state interactions. Results for color-suppressed $\overline{B}^0 \to D^{(*)0}X^0$ decays have been published by the CLEO collaboration [1]; however, only upper limits were obtained.

In this paper, we report on a search for the color-suppressed $\overline{B}^0 \to D^0X^0$, and $D^{*0}X^0$ decay processes, where the neutral meson X^0 is either a π^0, η, or ω. Charge conjugate modes are implicitly included in this paper. The data sample used in this analysis was collected with the Belle detector [2] at KEKB [3]. KEKB is a double storage ring with 8 GeV electrons and 3.5 GeV positrons colliding at a 22 mrad crossing angle. The data sample corresponds to an integrated luminosity of 21.3 fb^{-1} at the $\Upsilon(4S)$ resonance and contains 22.8 million $B\overline{B}$ pairs.

Belle is a general-purpose detector containing a 1.5 T superconducting solenoid magnet. Charged particle tracking covering 92% of the total center-of-mass (CM) solid angle is provided by a Silicon Vertex Detector (SVD) consisting of three concentric layers of double sided silicon strip detectors, and a 50-layer Central Drift Chamber (CDC). Particle identification is accomplished by combining the responses from an array of Silica Aerogel Čerenkov Counters (ACC) and a Time of Flight Counter system (TOF) with *dE/dx* measurements in the CDC. The combined response of the three systems provides at least 2.5σ K/π separation for laboratory momentum up to 3.5 GeV/c. Photons and electrons are detected in an array of 8736 CsI(Tℓ) crystals (ECL) located inside the magnetic field and covering the entire solid angle of the charged particle tracking system. The 1.5 T magnetic field is returned via an iron yoke that is instrumented to detect muons and K_L mesons (KLM). The KLM consists of alternating layers of resistive plate chambers and 4.7 cm thick steel plates.

For the light neutral meson X^0, we use the $\pi^0 \to \gamma\gamma$, $\eta \to \gamma\gamma$, $\eta \to \pi^+\pi^-\pi^0$ and the $\omega \to \pi^+\pi^-\pi^0$ decay channels. Charged tracks are required to have impact parameters that are within ± 5 cm of the interaction point along the positron beam axis and 1 cm in the transverse plane. We reject tracks that are consistent with electrons or muons. The remaining tracks are identified as pions or kaons according to a kaon to pion likelihood ratio. Candidate π^0 mesons are reconstructed from pairs of photons in the ECL that have an invariant mass within ± 16 MeV of the nominal π^0 mass [4]. The π^0 daughter photons are required to have energies greater than 50 MeV. Both photons from the $\eta \to \gamma\gamma$ mode are required to have $E_\gamma > 100$ MeV and the energy asymmetry of the daughter photons, $\frac{|E_{\gamma_1} - E_{\gamma_2}|}{E_{\gamma_1} + E_{\gamma_2}}$, is required to be less than 0.8. We remove η candidates if either of the daughter photons can be combined with any other photon with $E_\gamma > 100$ MeV to form a π^0 candidate. Candidate η mesons for the $\gamma\gamma$ mode are required to have an invariant mass within ± 10.6 MeV/c^2 ($\pm 2.5\sigma$) of the nominal η mass; the corresponding requirement for the $\pi^+\pi^-\pi^0$ mode is ± 3.4 MeV/c^2. Candidate η mesons are constrained to the nominal η mass; the fit also constrains the $\pi^+\pi^-$ pair from the 3π channel to a common vertex point. Candidate ω mesons are $\pi^+\pi^-\pi^0$ combinations with an invariant mass within ± 30 MeV/c^2 of the nominal ω mass value. The CM momentum of the π^0 from the ω decay is required to be greater than 350 MeV/c to reduce the large combinatorial background from low energy photons. The $\pi^+\pi^-$ pair from the ω decay is required to form a common vertex point within the beam interaction region

taking into account the lifetime of the B meson. Detailed studies of tracking, π^0 detection, and particle identification yield systematic errors in the detection efficiencies of 7.3% for prompt π^0, 6.6% for η, and 7.1% for ω mesons.

For candidate D^0 mesons we use the $D^0 \to K^-\pi^+$, $K^-\pi^+\pi^0$, and $K^-\pi^+\pi^-\pi^+$ decay modes. The CM momentum of the π^0 from $D^0 \to K^-\pi^+\pi^0$ decay is required to be greater than 300 MeV/c. The invariant mass of the D^0 candidates are required to be within $\pm 2.5\sigma$ of the measured D^0 mass, where σ is the D^0 mass resolution that varies between 5.5 and 13 MeV/c^2 depending on the decay mode. A mass and vertex constrained kinematic fit is then performed to the D^0 candidates. Good D^0 candidates are required to have an acceptable χ^2 value from the fit. D^{*0} candidates are reconstructed in the $D^{*0} \to D^0\pi^0$ decay mode. For these π^0 mesons, the photon energy cut is reduced to 20 MeV. For D^{*0} candidates, the mass difference, $\Delta m = M(D^0\pi^0) - M(D^0)$, is required to be within 2.5σ ($\sigma = 0.8$ MeV/c^2) of the nominal mass difference. The systematic error on the D^0 meson reconstruction efficiency is studied using the $B^- \to D^0\pi^-$ data sample. The error is determined to be 15% from a comparison of the observed number of signal events relative to the expected yield assuming the PDG $B^- \to D^0\pi^-$ branching fraction [4]. The systematic uncertainty in the detection efficiency for low momentum π^0s is found to be 10.7%.

We combine D^0s or D^{*0}s with X^0 meson candidates to form $\overline{B}^0$ candidates. Two kinematic variables are used to identify signal candidates, the beam-constrained mass $M_{bc} = \sqrt{(E^{\rm CM}_{\rm beam})^2 - (p^{\rm CM}_B)^2}$ and the energy difference $\Delta E = E^{\rm CM}_B - E^{\rm CM}_{\rm beam}$, where $E^{\rm CM}_B$ and $p^{\rm CM}_B$ are the CM energy and momentum of the $\overline{B}^0$ candidate, and $E^{\rm CM}_{\rm beam} = \sqrt{s}/2 \simeq 5.290$ GeV. The typical M_{bc} resolution is 3 MeV/c^2; the ΔE resolution ranges from 17 to 25 MeV, depending on the decay mode. When more than one $\overline{B}^0$ candidate is found in an event, the candidate with the minimum χ^2 is chosen, where $\chi^2 = \chi^2_{D^0} + \chi^2_{X^0}(+\chi^2_{\Delta m})$. Here $\chi^2_{D^0}$ is the χ^2 of the kinematic fit to the D^0, $\chi^2_{X^0}$ is the χ^2 of the kinematic fit to either the π^0 or the η. For the ω, $\chi^2_{X^0} = (\Delta(M_\omega)/\sigma(M_\omega))^2$, where σ is the measured resolution. For the $D^{*0}X^0$ modes, $\chi^2_{\Delta m}$, defined as $(\Delta(\Delta m)/\sigma(\Delta m))^2$, is included in the best candidate selection.

The background from continuum $e^+e^- \to q\overline{q}$ production is suppressed in the following ways. For the $D^{(*)0}\eta$ final state, we apply cuts on the ratio of the second to zero-th Fox-Wolfram moments [5], R_2, and the angle between the thrust axis [6] of the B candidate and the thrust axis of the rest of the event ($\cos\theta_T$). For the $D^{(*)0}\pi^0$ and $D^{(*)0}\omega$ final states, we use the B flight direction and a Fisher discriminant [7] containing several variables that quantify event topology [8]. We also use the D^{*0} helicity angle for the $D^{*0}\pi^0$ mode and the ω helicity angle and the ω decay amplitude for the $D^{(*)0}\omega$ mode [9]. Each of these variables is parameterized to form signal (S) and background (BG) probability density functions (PDF). The PDFs are multiplied to form a single likelihood $\mathcal{L}_{\rm S(BG)}$, and then a cut is applied on the likelihood ratio $\mathcal{L}_{\rm S}/(\mathcal{L}_{\rm S} + \mathcal{L}_{\rm BG})$ to suppress the $q\overline{q}$ background. Signal PDFs are determined using Monte Carlo (MC) and background PDFs are obtained from M_{bc} sideband data. The cut efficiencies are typically 70% and remove more than 90% of the $q\overline{q}$ background. The systematic error in the efficiency for this cut is determined by applying the same procedure to the $B^- \to D^{*0}\pi^-$ data sample. By comparing the cut efficiency between the data sample and MC, the systematic error is determined to be 5%.

In addition to the $q\overline{q}$ background, we observe large background contributions from color favored $B \to D^{(*)}(n\pi)^-$ decays and cross-talk from $D^{*0}X^0$ to D^0X^0 modes. The $D^{*+}\rho^-$ mode has the same final state as $D^0\omega$ and $D^0\eta$. However, when the D^{*+} daughter pion

is combined with the ρ^-, the invariant mass rarely falls within the ω or η mass window. The $D^{(*)0}\rho^-$ final state contaminates the $D^{(*)0}\pi^0$ mode if the ρ^- decays to a fast π^0. This mode also contaminates the $D^{(*)0}\eta$ channel if a photon from the fast π^0 is combined with another photon to form an η candidate. About half of these events are removed by explicitly reconstructing the $D^{(*)0}\rho^-$ final state. The contributions of these backgrounds in the η channel, as well as the feed-across from the $D^{(*)0}\pi^0$ mode, is also minimized by the π^0 veto discussed above. We also check for background contributions from $\overline{B} \to D^{(*)0}\rho'^-$ ($\rho'^- \to \omega\pi^-$) decays which have recently been observed by CLEO [10]. This two-body decay produces high momentum $D^{(*)0}$s and ωs that can fake signal events. Monte Carlo studies indicate that the remaining background events are shifted in ΔE by approximately the mass of the missing slow pion and thus can be distinguished from signal events by fitting the ΔE distribution.

The ΔE distributions for the various $D^{(*)0}X^0$ decays are shown in Fig. 2 after applying all selection cuts and requiring M_{bc} to be between 5.272 GeV/c^2 and 5.288 GeV/c^2. The signal is modeled with a Crystal-Ball function [11] with parameters obtained from MC. The background functions include a combinatorial component and a color-favored component. The D^0X^0 modes also include a component for cross-talk from color-suppressed $D^{*0}X^0$ modes. The combinatorial component is taken to be a second order polynomial with parameters determined by the ΔE shape in the M_{bc} sideband (5.20 GeV/c^2 $< M_{bc} <$ 5.26 GeV/c^2). The shapes of the color-favored and cross-talk components are modeled by MC histograms. The signal and background normalizations are free parameters in each fit.

Table I lists the signal yield, statistical significance, efficiency, and the branching fraction for each $D^{(*)0}X^0$ mode. The systematic errors due to fitting are obtained by varying the parameters of the fitting functions within 1σ of their nominal values. The change in the signal yield from each variation is added in quadrature to obtain the fitting systematic errors. These are typically 10%. The statistical significance is defined as $\sqrt{-2\ln(\mathcal{L}(0)/\mathcal{L}_{\rm max})}$ where $\mathcal{L}_{\rm max}$ is the likelihood at the nominal signal yield and $\mathcal{L}(0)$ is the likelihood with the signal yield fixed to zero. We observe signals for $\overline{B}^0 \to D^0\pi^0$, $D^0\omega$, and $D^{*0}\omega$ decays with more than 4σ significance. We find evidence of signals for $\overline{B}^0 \to D^{*0}\pi^0$, $D^0\eta$, and $D^{*0}\eta$ with more than 3σ significance. For decay modes with significance less than 4, we give 90% confidence level upper limits (UL) on the signal yields ($N_{\rm S}^{\rm UL}$) from the relation $\int_0^{N_{\rm S}^{\rm UL}} \mathcal{L}(N_{\rm S})\,dN_{\rm S} \,/\, \int_0^{\infty} \mathcal{L}(N_{\rm S})\,dN_{\rm S} = 0.9$, where $\mathcal{L}(N_{\rm S})$ denotes the maximum likelihood with the signal yield fixed at $N_{\rm S}$. The efficiencies for each decay mode are calibrated with control data samples. The final systematic errors include the errors in fitting, reconstruction efficiency, background suppression cut efficiency, and the number of $B\overline{B}$ pairs. Assuming the number of $B^0\overline{B}^0$ and B^+B^- pairs are equal, we calculate the branching fractions for various decay modes given in Table I. The branching fraction upper limits are calculated by increasing $N_{\rm S}^{\rm UL}$ and reducing the efficiency by their systematic errors.

In summary, using 22.8 million $B\overline{B}$ events collected with the Belle detector, we report the first observations of color-suppressed $\overline{B}^0 \to D^0\pi^0$ and $D^{(*)0}\omega$ decays. We also find evidence for $\overline{B}^0 \to D^{*0}\pi^0$ and $D^{(*)0}\eta$ signals. All the color-suppressed modes have similar branching fractions with central values between 1.4 and 3.4 $\times 10^{-4}$, as shown in Table I. In general, the branching fractions are consistently higher than recent theory predictions [12] based on the factorization hypothesis. This may be accounted for by additional corrections to the factorization models, or by non-factorizable effects such as final state interactions.

We wish to thank the KEKB accelerator group for the excellent operation of the KEKB accelerator. We acknowledge support from the Ministry of Education, Culture, Sports, Science, and Technology of Japan and the Japan Society for the Promotion of Science; the Australian Research Council and the Australian Department of Industry, Science and Resources; the Department of Science and Technology of India; the BK21 program of the Ministry of Education of Korea and the CHEP SRC program of the Korea Science and Engineering Foundation; the Polish State Committee for Scientific Research under contract No.2P03B 17017; the Ministry of Science and Technology of Russian Federation; the National Science Council and the Ministry of Education of Taiwan; the Japan-Taiwan Cooperative Program of the Interchange Association; and the U.S. Department of Energy.

REFERENCES

[1] CLEO Collaboration, T. Bergfeld, *et al.*, Phys. Rev. D **57**, 5363 (1998).

[2] Belle Collaboration, A. Abashian *et al.*, KEK Progress Report 2000-4 (2000), to be published in Nucl. Inst. and Meth. A.

[3] KEKB B Factory Design Report, KEK Report 95-7 (1995), unpublished; Y. Funakoshi *et al.*, Proc. 2000 European Particle Accelerator Conference, Vienna (2000).

[4] Particle Data Group, D.E. Groom *et al.*, Eur. Phys. J. **C15**, 1 (2000).

[5] G. Fox and S. Wolfram, Phys. Rev. Lett **41**, 1581 (1978).

[6] E. Farhi, Phys. Rev. Lett. **39**, 1587 (1977).

[7] R. A. Fisher, Annals of Eugenics, **7**, 179 (1936).

[8] We create a seven variable Fisher containing $\cos\theta_T$ and $S_\perp$, a variable that measures the momentum flow transverse to the X^0 direction. The next two variables, motivated by the original Fox-Wolfram moments, are defined as $r_l = (\Sigma_{i,j}|p_i||p_j|P_l(\cos\theta_{i,j}))/(\Sigma_{i,j}|p_i||p_j|)$ where i corresponds to a B candidate daughter particle and j corresponds to a particle not associated with the B candidate; p is the particle's momentum, P_l is a Legendre polynomial, $\theta_{i,j}$ is the angle between particles i and j, and l is either 2 or 4. The remaining three variables are equivalent in form to r_l with the exception that neither particles i or j are associated with the B candidate, $i \neq j$, and l corresponds to 2, 3, and 4.

[9] The D^{*0} helicity angle is defined as the angle between the D^{*0} flight direction and the direction of the D^{*0}'s daughter in the D^{*0} rest frame. The ω helicity angle is defined as the angle between the B flight direction and the normal to the ω decay plane in the ω rest frame. The ω decay amplitude is defined as the cross product of the two charged pions in the ω rest frame.

[10] CLEO Collaboration, J. Alexander, *et al.*, hep-ex/0103021, submitted to Phys. Rev. D.

[11] J. E. Gaiser *et al.*, Phys. Rev. D **34**, 711 (1986).

[12] M. Neubert and B. Stech, hep-ph/9705292, in *Heavy Flavours*, edited by A. J. Buras and M. Lindner, 2nd ed. (World Scientific, Singapore).

TABLE I. The obtained signal yield, statistical significance, efficiency including the sub-decay branching fractions, branching fraction ($\mathcal{B}$), and 90% confidence level upper limit (UL) for each $\overline{B}^0 \to D^{(*)0}X^0$ decay mode.

Mode	Signal Yield	Significance	Efficiency(%)	$\mathcal{B}$ ($\times 10^{-4}$)	UL ($\times 10^{-4}$)
$D^0\pi^0$	$127.6\ ^{+18.5\ +11.6}_{-17.9\ -12.5}$	7.9	1.93	$2.9\ ^{+0.4}_{-0.3} \pm 0.6$	–
$D^{*0}\pi^0$	$17.1\ ^{+6.6\ +1.6}_{-5.9\ -2.4}$	3.2	0.49	$1.5\ ^{+0.6\ +0.3}_{-0.5\ -0.4}$	2.3
$D^0\eta$	$25.7\ ^{+8.4\ +3.0}_{-7.7\ -2.8}$	3.8	0.79	$1.4\ ^{+0.5}_{-0.4} \pm 0.2$	2.1
$D^{*0}\eta$	$7.7\ ^{+3.4\ +0.7}_{-2.7\ -0.8}$	3.6	0.22	$1.5\ ^{+0.7}_{-0.6} \pm 0.4$	2.7
$D^0\omega$	$30.2\ ^{+8.6\ +3.1}_{-7.8\ -3.4}$	4.7	0.80	$1.7\ ^{+0.5\ +0.3}_{-0.4\ -0.4}$	–
$D^{*0}\omega$	$17.7\ ^{+6.5\ +2.3}_{-5.8\ -2.2}$	4.3	0.23	$3.4\ ^{+1.3}_{-1.1} \pm 0.8$	–

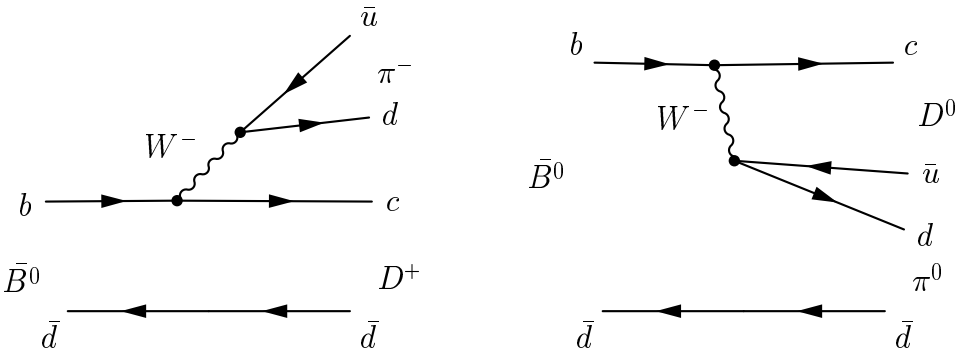

FIG. 1. The external(left) and internal(right) spectator diagrams for $\overline{B} \to D\pi$ decays.

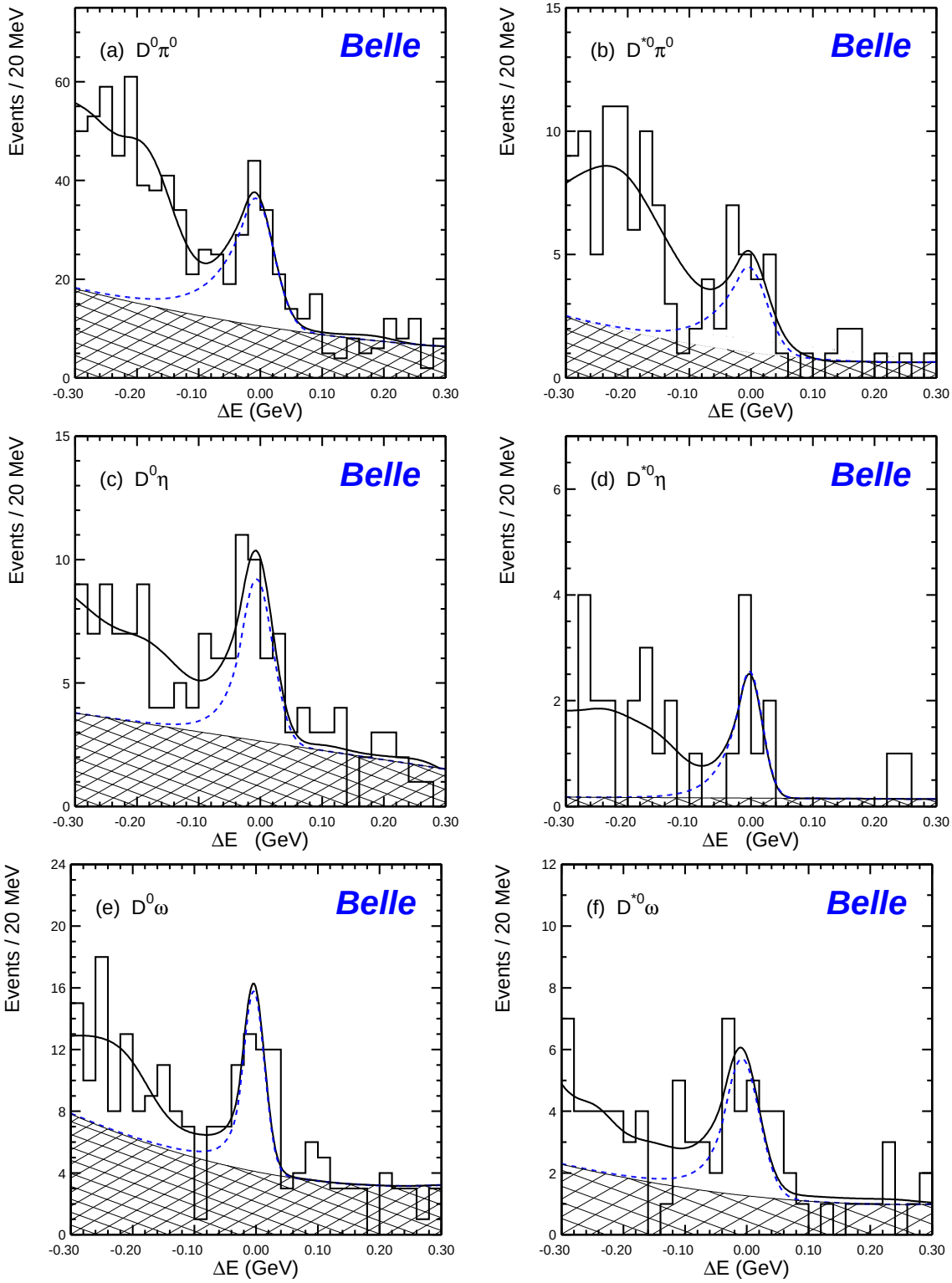

FIG. 2. The ΔE distribution for (a) $D^0\pi^0$, (b) $D^{*0}\pi^0$, (c) $D^0\eta$, (d) $D^{*0}\eta$, (e) $D^0\omega$, and (f) $D^{*0}\omega$. The solid line shows the fitting result. The dashed line shows the sum of the signal component and the combinatorial background component. The combinatorial component is shown separately as the cross-hatched area.